Journal of Magnetism and Magnetic Materials 380 (2015) 61–65

Contents lists available at ScienceDirect

Journal of Magnetism and Magnetic Materials

journal homepage: www.elsevier.com/locate/jmmm

Optical detection of nanoparticle agglomeration in a living system under the influence of a magnetic field

Robert Müller [a,*], Ondrej Stranik [a], Florian Schlenk [b], Sebastian Werner [b], Daniéll Malsch [a], Dagmar Fischer [b], Wolfgang Fritzsche [a]

[a] Leibniz Institute of Photonic Technology, Albert-Einstein-Str. 9, 07745 Jena, Germany
[b] Department of Pharmaceutical Technology, Institute of Pharmacy, Friedrich Schiller University, Otto-Schott-Str. 41, 07745 Jena, Germany

ARTICLE INFO

Article history:
Received 18 June 2014
Received in revised form
8 October 2014
Accepted 9 October 2014
Available online 18 October 2014

Keywords:
Magnetic particles
Chick area Vasculosa
Particle transport
Agglomeration

ABSTRACT

Nanoparticles are important in diagnosis and therapy. In order to apply their potential, an understanding of the behavior of particles in the body is crucial. However, *in vitro* experiments usually do not mimic the dynamic conditions of the *in vivo* situation. The aim of our work was an *in vivo* observation of particle transport in chicken egg vessels in the presence of a magnetic field by particle tracking. For that we demonstrate the spatial resolution of our observations in a vein and a temporal resolution by observation of the cardiac cycle in an artery. Microscopic images were recorded in dark field reflection and fluorescence mode.

1. Introduction

Manufactured particles are attracting increasing importance in diagnosis, for drug delivery in therapy as well as in prevention [1,2]. Differences between the *in vitro* test conditions under static conditions e.g. in cell culture, and the dynamic *in vivo* conditions in the blood stream were suggested as one of the reasons for the low number of particle applications making their way through clinical to the market [3]. Blood flow may compromise the interaction between the particles and their targets. Most of the *in vitro* experiments do not mimic the dynamic conditions of the *in vivo* situation, therefore real-life extrapolations are challenging.

Chicken-based test systems using eggs and embryos represent one option for medical and toxicological research exploring nanoparticle *in vivo* behavior, but were only rarely employed [4]. So information about the use of hen egg models as *in vivo* test system to investigate the flow conditions of manufactured particles is still limited.

Blood flow has exceptional rheological properties which are due to blood composition consisting of plasma and cellular components, mainly red blood cells (RBCs). The deformation and orientation of RBCs and their ability to form rouleaux in the absence of shear stress are the key cellular factors affecting blood viscosity [5]. So far, the blood flow in the presence of nanoparticles has mainly been studied using theoretical flow simulations or artificial microchannel systems [6]. It was shown that red blood cells are moving substantially in the center of the blood stream and are showing a tumbling effect. By volume displacement and the tumbling effect of RBCs the concentration of nanoparticles is increased in the peripherial areas of the vessels [6].

The existing velocimetry studies on chick embryo were performed on candled eggs, where the eggs are backlighted by a bright light source and details show through through the shell [7,8]. It utilized μPIV (micro particle imaging velocimetry), a method for the characterization of flow conditions based on the imaging and correlation investigations of consecutive frames. These studies were focused on the calculation of wall shear stress forces. For artificial tracers like liposomes or polystyrene microparticles, fluorescence microscopy is necessary. The artificial tracers have to be injected intravenously with a glass micro needle by penetration of the vitelline membrane.

The influence of the magnification as key optical parameter in μPIV measurements was investigated for particle transport in chicken egg vessels [9]. Deviations in the measured velocities of blood cells and fluorescent polymer beads at different magnifications increase with higher magnification, caused by differences between centerline velocity and depth-averaged velocity. A magnification $< 15\times$ is recommended.

In [10] a study of the dynamics of CdSe/ZnS quantum dots and polystyrene nanospheres in the blood vessels of the chicken embryo chorioallantoic membrane was undertaken.

* Corresponding author.
E-mail address: robert.mueller@ipht-jena.de (R. Müller).

http://dx.doi.org/10.1016/j.jmmm.2014.10.043
0304-8853/

The transport of magnetic particles in rat blood vessels was observed macroscopically using a small distance between magnetic field source (permanent magnet) and particles [11]. Three transport modes of MNP in vessels could be distinguished: velocity dominated, magnetically dominated, and a boundary layer formation. The latter one occures already in the presence of magnetic forces (by an external magnetic field gradient) of about 0.005% of the centerline drag forces (by blood flow). In the considerations a constant hydrodynamic size, i.e. no agglomeration, was assumed.

Aim of our work is the first *in vivo* observation of magnetic particle transport in chicken egg vessels in presence of a magnetic field by single particle tracking (SPT). For that we demonstrate the spatial resolution of our observations by means of non-magnetic fluorescence beads.

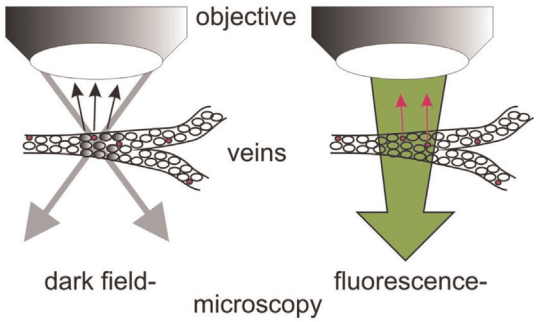

Fig. 1. Scheme of the detection modes: observation of erythrocytes and vessel topology by scattering in dark field illumination (left) and observation of fluorescence labeled particles (red) after excitation. (For interpretation of the references to color in this figure legend, the reader is referred to the web version of this article.)

2. Materials and methods

For the HET-CAV (hen's egg test–chick area vasculosa), fertilized eggs of White Leghorn chicken were incubated at 37 °C and at 80% relative humidity in horizontal position. After 72 h, the eggs were poured into a Petri dish containing Ringer solution and incubated for further 24 h. Particles (25 mg/ml) were injected intravenously with a borosilicate glass capillary (World Precision Instruments, Inc., Sarasota, USA) at a volume of 1 μL using a micromanipulator MM33-R (Märzhäuser Wetzlar GmbH, Wetzlar, Germany) and a dosing volume XenoWorks microinjector (BRI 217; Sutter Instrument Co., Novato, USA) connected to a 100 μL syringe (Hamilton, Bonaduz, Switzerland). Only embryos with an intact yolk sac membrane, well-developed blood vessels and constant heart beat (0.5 Hz), were selected for the experiments. Immediately after particle injection the embryos were transferred to the microscope for flow analysis.

Two different types of particles with different physicochemical properties were used for the biological tests. Commercially available carboxylate-modified polystyrene latex beads, (L4530, Sigma-Aldrich, Germany) with a diameter of 2 μm were compared to fluorescent-labeled superparamagnetic iron oxide nanoparticles (SPIONs) with starch coating with a hydrodynamic size of 150 nm (nano-screenMAG/R-D, chemicell GmbH, Berlin, Germany), according to the suppliers information. The latex beads had a fluorescence extinction maximum and emission maximum at 470 and 505 nm, respectively. The magnetic particles showed their maxima at 578 and 613 nm.

Hydrodynamic diameter (HD) and polydispersity index (PDI) of the magnetic particles were measured at a concentration of 0.05 mg/ml by photon correlation spectroscopy (PCS) at 25 °C with a Zetasizer Nano ZS (Malvern Instruments, Herrenberg, Germany) using the Zetasizer software 7.02. The viscosity (0.8872 mPa s) and the refractive index (1.330) of distilled water and the refractive index (2.420) of iron oxide at 25 °C were used for analysis of the data. Results were calculated from three independent samples with each sample measured in five runs. Zeta potential measurements were carried out under the same conditions in a standard capillary electrophoresis cell (DTS1070, Malvern Instruments) of the Zetasizer Nano ZS.

Optical images were recorded with an optical microscope AxioImager Z1.m (Carl Zeiss, Jena, Germany) using a tungsten lamp and a PCO Sensicam camera. The microscope is operated in the dark field reflected light and fluorescence mode, respectively (see Fig. 1). The scattered light was captured only from a measuring spot that scales with the magnification of the microscope. In combination with a 5× objective the observed area had a diameter of about 1.7 mm. The picture size is 688/520 (horizontal/vertical) pixel. One pixel of the video corresponds to 2.58 μm of the object. The used camera settings are: Gain setting: normal, Binning horz./vert.: 2/2, Delay: 0 ms, Exposure: 40 ms.

Analysis is realized with TrackMate [12], a versatile SPT plugin for the image processing package Fiji [13]. It performs image segmentation, feature-based filtering, particle-linking and the visualization of the results. We employ the built-in LoG (Laplacian of Gaussian) filter for image segmentation. Tracking is based on the LAP tracker (Linear Assignment Problem) [14] with splitting and merging activated where applicable. Spots and tracks are filtered in order to exclude stagnant particles and uncertain results.

3. Results and discussion

In previous studies the blood flow in heart [7] and blood vessels [9] of chicken embryos has been studied using fluorescent artificial tracers injected into a candled egg placed in a water bath. In the present work, we selected a different setup using a shellless, planar embryo model demonstrating several advantages. The planar surface of the open egg model made the whole blood circulation accessible for investigation. Incubating the embryo in open conditions, the same vessels can be investigated for several hours to days. The velocimetry measurements are focused on the particle speed distribution over the vessel.

Erythrocyte aggregation and hemolysis depending on the particle concentration were investigated in order to see possible effects that could alter the transport properties.

The hemocompatibility of the particles indicated their suitability for administration directly into the systemic circulation. The hemolytic behavior of the particles was tested according to the ASTM F756-08 standard [15]. None of the particles did show any detectable disturbance of the red blood cell membranes (hemolysis $<2\%$) under the chosen conditions. No aggregation of red blood cells was induced by particles up to 10-fold higher concentration than reached in the embryo model (data not shown).

The hydrodynamic diameter measured by photon correlation spectroscopy was 191 ± 2 nm with a polydispersity index of 0.207 ± 0.008. The zeta potential was -5.5 ± 0.4 mV.

The behavior of the magnetic particles in a flowing medium exposed to an external magnetic field was investigated in a microfluidic channel in order to see whether particles form agglomerates irreversibly caused by magnetic interaction. The results are described below.

In vivo transport experiments in the absence of a magnetic field were done with carboxylate-modified polystyrene latex beads. In Fig. 2 (top) a dark field image revealing a large vein, smaller vessels and the red blood cells as well as a fluorescence image with the latex beads are shown. The width of the image is about

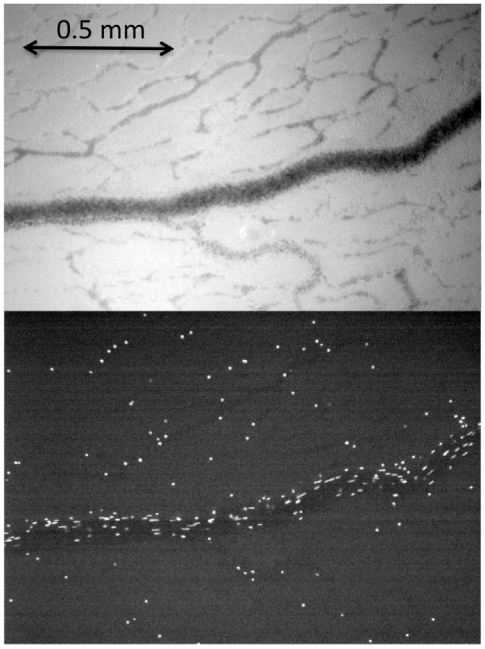

Fig. 2. Still frames of the flow in a vein demonstrate the spatial resolution: dark field image (top), fluorescence image (bottom).

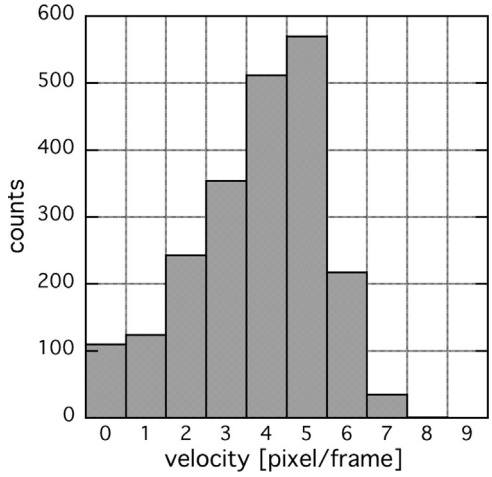

Fig. 3. Velocity distribution of the particles determined from the fluorescence image Fig. 2 (1 pixel/frame ≈ 50 μm/s).

1.6 mm. Most particles (in the large vein) have a velocity of ≈ 200 μm/s (Fig. 3).

Fig. 4 shows fluorescence images of an artery with tracked objects during diastole and systole, i.e. minimum and maximum velocity of the particles. The velocity is illustrated by the length (20 frames) and coded by the color of the "tails" (blue: low velocity).

Transport experiments in the presence of a static magnetic field were done with starch-coated superparamagnetic beads of 150 nm size (nano-screenMAG/R-D). Because of the small size of the initial magnetic beads, a particle tracking of single particles is not possible. Only agglomerates were tracked and their growing and velocities could be seen, what might give a qualitative impression. The magnetic field was generated by a cylindrical NdFeB magnet that was placed near the objective. From magnetic field simulations, the field parameters at the region of interest were estimated to be B=40 mT and gradB=5 T/m. In such a magnetic field, superparamagnetic beads dispersed in water tend to agglomerate reversibly, i.e. after removing the field the agglomerates should

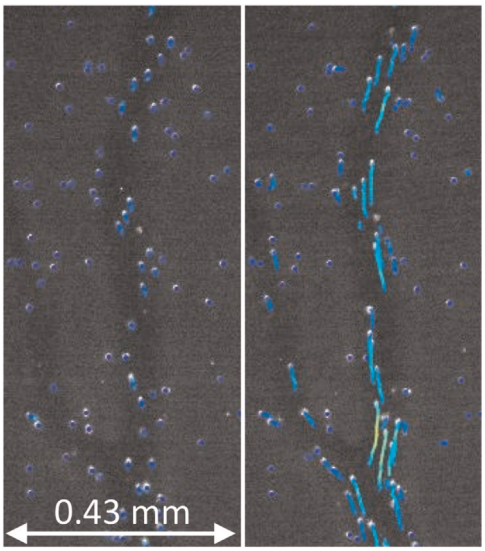

Fig. 4. Still frames (fluorescence contrast) of the flow in an artery show the temporal resolution in the tracking analysis (right): "tails" are 20 frames long. (For interpretation of the references to color in this figure, the reader is referred to the web version of this article.)

dissolve into single beads again by Brownian motion if there is no non-magnetic interaction between the particles. This behavior of the magnetic particles in a flowing medium exposed to an external magnetic field was confirmed in a microfluidic channel (cross section 260 × 300 μm^2, flow rate 5 μl/min). The particles were dispersed in water with a concentration of about 2.5 mg/ml. Fig. 5 shows the formation of agglomerates after switching on the field, visible as bright white speckles in the channel structure (Fig. 5b). A gradient of the field causes a magnetic force, i.e. a movement of particles in direction of the higher field strength. The force can be estimated based on the product that results by multiplying the magnetic moment dependent upon the field strength and the field gradient dependent upon distance from the magnet. Fig. 5d reveals the transport of the agglomerates into direction of the higher field gradient (to the left) after some seconds. Here they form a sediment. After switching off the field (Fig. 5d) the aggregates in the flowing volume start to dissolve immediately, however the sediment needs about 10 s to be washed away.

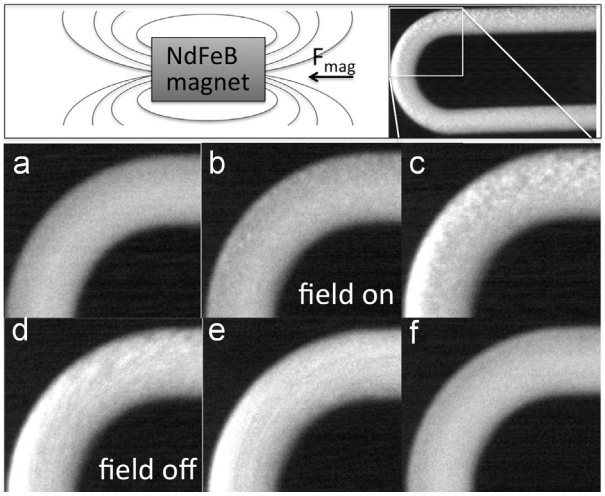

Fig. 5. Influence of a magnetic field on the flow of magnetic particles in a microfluidic channel: fluorescence images before field (a), immediately (b) and 4s (c) after switching on the field, immediately (d), 2s (e) and 12s (f) after switching off the field. (channel width: 300 μm).

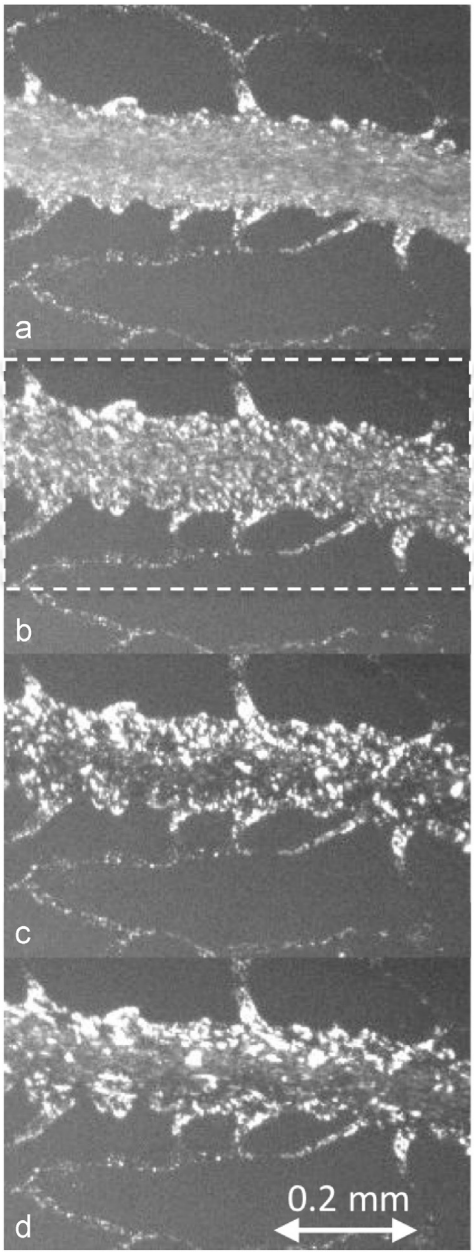

Fig. 6. Influence of magnetic field on the flow of magnetic particles in a vein: fluorescence images before field (a), after 4 s field (b), after 10 s field (c), 8 s after removing the field (d).

Analogeous experiments were carried out *in vivo* after injection of particles into a vein. Fig. 6 shows fluorescence images of a vein before applying a field (a), after about 4 s (b) and 10 s (c) applying a field, and 8 s after removing the field (d). Since the magnetic force is not aligned with the flow direction (in Fig. 6 slanted to the top and slightly above the image plane) it causes a hydrodynamic resistance what leads to a decreasing velocity or even stopping of the particles near the vascular wall.

The images reveal a strong agglomeration caused by magnetic forces. A magnetic field (even in case of ideal superparamagnetic particles) leads to the formation of magnetic agglomerates, i.e. particles come in close contact induced by magnetic forces. After removing the field, the agglomerates move again, sometimes even faster. However, there is only a partial dissolving of the agglomerates, in contrast to the particles behavior in the microfluidic channel. This leads to interaction of nanoparticle coating and may cause an irreversible agglomeration. Particles entering the

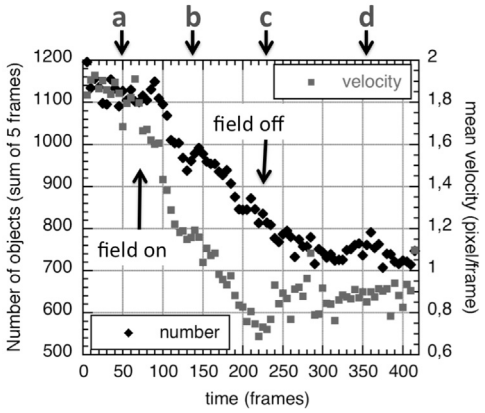

Fig. 7. Number of tracked objects (sum of 5 frames) and their mean velocity versus time. a–d: see Fig. 6.

viewable area later than 8 s after removing the field seemed less agglomerated than in Fig. 7d but more than in Fig. 7a.

The number of tracked objects (inside the dashed frame) stays almost constant, however the velocity seems to increase a little (Fig. 7). The data show only a tendency. One single particle is too small for an observation so that a merging and splitting of objects would not be detected properly.

Some agglomeration of the particles is observed even before applying the magentic field (Fig. 6a). When nanoparticels enter the blood stream, e.g. by systemic administration, interactions with blood cells such as erythrocytes and thrombocytes will occur and blood proteins bind immediately to the nanoparticle surface. These effects may lead to the formation of larger agglomerates.

A further characterization of agglomerate formation in a magnetic field was done by image processing without particle tracking. After binarization of the four freeze frames a distribution of the size of the identified objects were determined (Fig. 8) for all objects bigger than one pixel. We found an increased size of agglomerates with increasing frame number. However, this method is hindered by the missing resolution of objects smaller 1 pixel (2.58 μm).

A selected area inside the vessels was analyzed with respect to the gray value distribution (Fig. 9). This gives an information about the "concentration" of particles or agglomerates that can not be dissolved by our optical system during observation. The measurements reveal an increasing separation of the gray values with increasing frame number. The formation of a population of white pixel corresponds with that of the agglomerates. After switching off the magnetic field, a shift of the main peak to brighter values

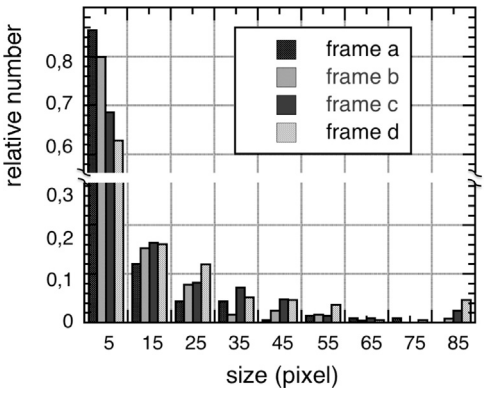

Fig. 8. Distribution of the size of objects (agglomerates) in the frames of Fig. 6a–d depending on the presence of a magnetic field. (1 pixel=2.58 μm).

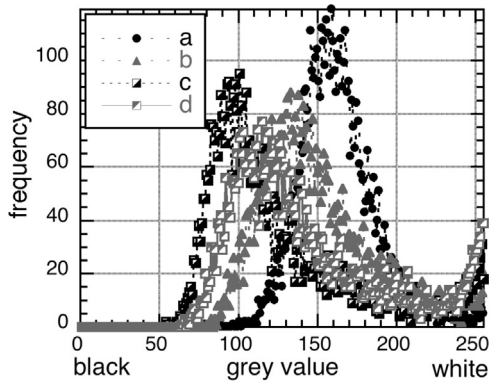

Fig. 9. Gray value distribution inside the vessel in Fig. 6a–d.

can be seen, what can be interpreted as a partly dissolving of small agglomerates.

Nevertheless, if we assume superparamagnetic behavior, the keeping of agglomerates after removing the magnetic field could be caused by surface interaction with blood components depending on the coating of the particles. Examples of the influence of the coating are given in [16] and [17].

In the future work, experiments based on the method described in this paper will focus on the establishment of a prediction model for the development of nanoparticulate systems like contrast agents, drug delivery systems, and theranostics with improved hemocompatibility and flow distribution profiles. The model could allow the prediction of clinically critical events (embolism and thrombosis) in an early phase of nanoparticle development without performing an animal experiment. As an advantage compared to mammalian animal experiments, a huge amount of new test materials can be tested as high-througput strategy. The hen egg model is easy to perform, time- and material-saving without limits from ethical and legal points. Additionally, costs are low compared with mammalian models.

4. Conclusion

Hen's egg models are known as suitable models for blood flow analysis of blood cells and artificial tracers. The shell-less HET-CAV model is an advantageous system by offering a planar surface making the entire embryonic blood circulation optically accessible. Further advantages are the easy injectability and the possibility to investigate objects up to 48 h.

The transport of magnetic particles in chicken egg vessels can be microscopically observed under the influence of a magnetic field in dark field reflected light and fluorescence mode combined with single particle tracking (SPT). The observed irreversibility of agglomerates after removing the magnetic field suggests a surface interaction of particles with blood components depending on the coating of the particles.

Acknowledgments

The authors would like to acknowledge Ch. Bergemann (chemicell GmbH, Berlin) for providing the magnetic particles, A. Herre (FSU) for excellent technical assistance and G. Nowak (FSU) for support with the CAV model.

The work was supported by BMBF Grant 03X0104D and E, project “NanoMed”.

References

[1] W.H. De Jong, P.J. Borm, Drug delivery and nanoparticles: applications and hazards, Int. J. Nanomed. 3 (2) (2008) 133–149.
[2] S. Parveen, R. Misra, S.K. Sahoo, Nanoparticles: a boon to drug delivery, therapeutics, diagnostics and imaging, Nanomedicine 8 (2) (2012) 147–166.
[3] M.A. Dobrovolskaia, S.E. McNeil, Understanding the correlation between in vitro and in vivo immunotoxicity tests for nanomedicines, J. Control Release 172 (2) (2013) 456–466.
[4] A. Vargas, et al., The chick embryo and its chorioallantoic membrane (CAM) for the in vivo evaluation of drug delivery systems, Adv. Drug Deliv. Rev. 59 (11) (2007) 1162–1176.
[5] O.K. Baskurt, H.J. Meiselman, Blood rheology and hemodynamics, Semin. Thromb. Hemost 29 (5) (2003) 435–450.
[6] J. Tan, A. Thomas, Y. Liu, Influence of red blood cells on nanoparticle targeted delivery in microcirculation, Soft Matter 8 (2011) 1934–1946.
[7] P. Vennemann, et al., In vivo micro particle image velocimetry measurements of blood-plasma in the embryonic avian heart, J. Biomech. 39 (7) (2006) 1191–1200.
[8] C. Poelma, et al., In vivo blood flow and wall shear stress measurements in the vitelline network, Exp. Fluids 45 (4) (2008) 703–713.
[9] C. Poelma, et al., Accurate blood flow measurements: are artificial tracers necessary? PLoS One 7 (9) (2012) e45247.
[10] A.A. Clancy, Y. Gregoriou, K. Yaehne, D.T. Cramb, Measuring properties of nanoparticles in embryonic blood vessels: towards a physicochemical basis for nanotoxicity, Chem. Phys. Lett. 488 (2010) 99–111.
[11] A. Nacev, C. Beni, O. Bruno, B. Shapiro, Magnetic nanoparticle transport within flowing blood and into surrounding tissue, Nanomedicine 5 (9) (2010) 1459–1466.
[12] ⟨http://fiji.sc/TrackMate⟩.
[13] ⟨http://fiji.sc/Fiji⟩.
[14] K. Jaqaman, et al., Robust single-particle tracking in live-cell time-lapse sequences, Nat. Methods 5 (8) (2008) 695–702.
[15] ASTM F756, 2000 (2008). Standard Practice for Assessment of Hemolytic Properties of Materials. In: Annual Book of ASTM Standards, Vol. 13.01. Philadelphia: ASTM; 2008.
[16] D. Eberbeck, et al., Quantification of the aggregation of magnetic nanoparticles with different polymeric coatings in cell culture medium, J. Phys. D: Appl. Phys 43 (2010) 405002 (9p.).
[17] Müller, Robert, et al., In situ measurements of magnetic nanoparticles after placenta perfusion, J. Magn. Magn. Mater., in print, http://dx.doi.org/10.10%2016/j.jmmm.2014.09.072.